Interactive comment on "Characterization of long-range transported Saharan dust at the Caribbean by dual-wavelength depolarization Raman lidar measurements" by S. Groß et al.

Anonymous Referee #1
Received and published: 3 August 2015

We thank this Reviewer for his careful reading of the manuscript and for his suggestions to help us improve the paper.

The answers are given in a direct response (bold, italic).

The paper by Groß and Co-authors presents optical properties of Saharan dust layers over Barbados that have been derived from lidar observations conducted in the framework of SALTRACE, the follow-up to the highly successful SAMUM campaigns. The authors show that lidar-derived intensive properties of Saharan dust at the Carribean show negligible difference to observations closer to the source regions and in Central Europe. The paper presents solid findings that are of interest to the readers of ACP. However, I suggest major revisions before publication because I believe that the findings could be presented more concisely if the paper was freed of unnecessary ballast.

Major points:

- I suggest significant restructuring of the paper. The presentation of four case studies is excessive and should be revised. Additional cases do not provide additional information - particularly as the observed properties don't vary much. I suggest to stick to one or (at most!) two case studies.

  We decided not to reduce our results to just one or two case studies. One main topic of our study is if different dust mobilization mechanisms, found for the SALTRACE period and are discussed in the text, have an impact on the optical properties of long-range transported Saharan dust. For the four case studies we found no significant differences in the optical properties measured by lidar at Barbados.

- The number of figures exceeds what I would consider reasonable for the amount of text. For instance, Figure 1 is redundant as it doesn't help in understanding the measurement capabilities of POLIS. It is also unnecessary to present identical information multiple times. For instance, basically the same statistics are provided in Table 1 and Figures 13, 14, and 15. In the same way Table 2 overlaps with what is presented in Figures 14 and 15. Please decide on presenting your findings either as figure or as table and omit what is not needed from the paper.

  The large number of figures results from the number of case studies we discuss in this work. But we agree with this referee that there is some potential to tighten the information. For this reason we removed Figure 1 and 13. However we want to keep Figures 14 and 15 additionally to the information provided in Tables 1 and 2.

- You might make better use of the information in Figures 3 and 4 by combining trajectories and source regions for individual cases in a single figure for the example case you decide to present in the revised paper. The discussion of the measurement period (e.g. discussion of Figure 2) could still include which source regions have been active during which part of the campaign.

We also thought about this but finally decided to present the results in a more compact way and keep the current presentation of the data; especially as a different presentation of the data would result in 2 additional figures.

- Why do the profiles of lidar ratio and PLDR not cover lower heights when statistical information on the parameters at these heights is given later in Table 1 and in Figures 13 and 16?

We included the lower height ranges in the profiles.

- It is incredible to see that the optical properties of Saharan dust remain unchanged after thousands of kilometers of transport. Can you speculate about possible aging and transport effects (mentioned on page 19339,lines 20-24) based on the data presented in the paper? Regarding the argument made there (effect of transport path): Are the source regions for the measurements at Munich similar to those active during SAMUM and SALTRACE?

We agree with this referee that it is astonishing to find almost unchanged optical properties for long-range and fresh Saharan dust. We are still working on this topic and do not want to make hasty speculations so far. Furthermore, similar dust source regions were active for the Munich dust event and our measurements at Barbados.

Minor points:

- the city in affiliation 3 should be Valladolid

This was a typo. We changed it.

- I think the title does not properly reflect the content of the paper. The authors do not present a complete characterization of the observed dust layers (i.e. including microphysical and chemical properties of the particles). They focus on optical properties only. I therefore suggest revising the title. What about "Optical properties of Saharan dust over Barbados as measured with dual-wavelengths depolarization Raman lidar"

We followed this reviewer's suggestion and changed the title accordingly.

- Please don't use acronyms without proper introduction, e.g. AOD and SALTRACE in the Abstract.

We changed that.

- Always give the wavelength when discussion AODs or AEs.

We added the wavelength to all discussions of AOD and AE.

- p19326,l4 and p19326,l13: "at the end of its way across the Atlantic" is kind of misleading. Who says that the dust isn't transported any further west? I suggest changing this to after transport across the Atlantic

We changed that.

- p19327,l5/6: sentence is redundant

We removed this sentence.

- p19327,l8: please provide original references to HSRL

We changed the references.

- p19327,l13: note that CATS, currently flying on the ISS, is equipped with a HSRL channel at 532nm

We included CATS in the introduction.

- p19330,l11: What is meant with "high accuracy"?

This is redundant; we removed it at this point.

- Section 2.3 Data evaluation should be called Data analysis

We changed that.

- p19330,l25: Raman channels "during daytime"

We added "during daytime".

- p19331,l2: validated by "assessing the temporal evolution of the range-corrected signal" over the smoothing period

We changed that.

- p19331,l4 and later: please give smoothing lengths in meter, range bins should be in parentheses

We changed that.

- p19331,l9: What makes this method highly accurate? You cannot just state this.

The high accuracy of this method is demonstrated in the referenced publication. However, to avoid misunderstandings we removed "highly accurate" at this point.

- p19333,l8-13 and l17-22: Shouldn't this be part of Section 2?

We moved these paragraphs to Section 2.

- p19335,l1-4 (and the other case studies): Why is this not shown as profiles in Fig. 6 (8, 10, 12)?

We included the PLDR of the lowermost layer in Fig. 6, 8, 10, 12.

- p19340,l26: What are the threshold values for those aerosol types in the EarthCARE classification scheme? It might be worthwhile to add those to Figure 16. This would be useful information when getting to the end of this paragraph: "Thus, this threshold has to be adapted..."

We did not add the threshold in Figure 16, but we added the values in the text.

- p19341,l20: closely related? what does this mean?

We changed "closely related with former measurements" to "follow up former measurements".

Interactive comment on “Characterization of long-range transported Saharan dust at the Caribbean by dual-wavelength depolarization Raman lidar measurements” by S. Groß et al.

Anonymous Referee #2
Received and published: 31 August 2015

We thank this Reviewer for his careful reading of the manuscript and for his suggestions to help us improve the paper.

The answers are given in a direct response (bold, italic).

This paper presents aerosol optical properties derived from high quality lidar observations during SALTRACE, the Saharan Aerosol Long-range Transport and Aerosol-Cloud interaction Experiment. Detailed presentation of several Saharan dust intrusions cases including the particle linear depolarization ratio at both wavelengths is well done. I found very useful the analysis of the active dust sources relevant for the four investigated case studies and I appreciate as an important issue the presentation of the profiles and RCS in all four cases. I think the paper is a substantial contribution to scientific progress within the scope of Atmospheric Chemistry and Physics. The description of experiments and calculations is sufficiently complete and precise to allow their reproduction by other scientists. The results are discussed in an appropriate and balanced way. The authors give proper credit to related work and clearly indicate their own contribution. I am suggesting only few minor changes as follows:

- Figure 1- Please provide a technical drawing instead of the picture of the instrument.

  We removed Figure 1.

- In the abstract please rephrase “long-range transported Saharan dust at the end of its way across the Atlantic”- this one sounds like you have a proof the dust get deposited in Barbados or somehow vanished after crossing the Atlantic

  We changed “at the end of its way across the Atlantic” to “after transport across the Atlantic”.

- Please rephrase also this statement “Our study includes the general aerosol situation during our measurement period as well”- I am not sure what you meant by ”general aerosol situation”.

  We changed this statement to “… a general investigation of aerosol layering and optical depth …”.

Interactive comment on “Characterization of long-range transported Saharan dust at the Caribbean by dual-wavelength depolarization Raman lidar measurements” by S. Groß et al.

AM Miffre
Received and published: 8 September 2015

We thank Dr. Miffre for his suggestions to help us improve the paper.

The answers are given in a direct response (bold, italic).

The manuscript proposed by S. Groß et al. reports on lidar measurements performed in the Caribbean Island of Barbados. The introduction states the difficulty of studying dust particles after long-range transport and underlines the complexity of involved atmospheric processes such as aging, mixing with other aerosols or nucleation to quote only a few. Facing such a complexity is indeed difficult while ideally lidar measurements should become standard tools for atmospheric studies. In this context, all my comments are intended to improve the science of this manuscript and help potential future readers.

On the methodology
The methodology proposed by S. Groß et al. to analyze two-component particle mixtures is not the only existing one nor the pioneering one. As the manuscript may potentially have a large impact, other methodologies (Shimizu et al. JGR2004, Nishizawa et al. JGR2007, David et al. ACP2013) could be quoted, especially in a context where more than 45 % of the given references are from one of the co-authors.

We do not claim to develop a new methodology for data analyzing, but we use an established procedure which (for our measurements) is described in the referenced literature and apply it, for the first time, to lidar measurements of long-range Saharan dust at Barbados. This method is based on a long history of data analysis. As this history might be of interest for readers we included some more references in the text.

On the measurements and the analysis
How is the PLDR-value and uncertainty of 0.27 ± 0.01 retrieved from the measurements? Looking at the observed vertical profiles, the uncertainty seems larger. Accordingly, how does the “highly accurate ±45_ calibration method” (page 19331, line 9) relate with other published methods (Alvarez et al. JTECH2006, David et al., APB2012) that rely on a dozen of points ?

We guess that the comment refers to Figure 8 and Table 1. Indeed the error bars are too large in the figure by mistake. The data in Table 1 are correct. We changed Figure 8. As mentioned in the text, "the error calculation of δv and δp was done analogue to Freudenthaler et al. (2009)". For the determination of the calibration factor V*, or G, Alvarez et al. (JTECH 2006) and David et al. (APB 2012) use a halve wave plate to rotate the plane of polarization of the light in the receiving optics by angle φ, while POLIS uses a mechanical rotation of the receiving optics. For both methods Eq. 10 in Freudenthaler et al. (Tellus 2009) shows that the signal ratio of the cross and the parallel channels δ*, from which the calibration factor V* is determined, depends on φ and on the volume linear depolarization ratio δv, except for φ = ±45°, where the dependence on δv vanishes. Actually only one measurement of δ* at φ = +45° or -45° would be necessary to determine V*, but usually the plane of polarization of the laser beam and the absolute position of the calibrator rotation are not exactly known, which introduces another parameter γ, the offset angle, which is considered in Alvarez (JTECH 2006) but not mentioned in David (APB 2012). That means in general three

parameters have to be retrieved, which requires at least three measurements at different angles. The measurements of δ* around 0° and 90° are most sensitive to δv and least around ±45°, while the sensitivity to γ is highest around ±45° and lowest around 0° and 90. For the latter problem it is shown by Freudenthaler et al. (Tellus 2009) with a numerical simulation (it can also be shown analytically), that the geometric mean of two measurements around ±45° exactly 90° apart the influence of δv and γ are decreased by a factor of about 100, which reduces the number of necessary measurements again to two. Another reason for using as few as possible measurements is the signal to noise ratio, which increases with averaging time and vice versa decreases with the number of measurement points for a given time for the whole calibration. This is important because the calibration should be done regularly (we do it every time we switch on the lidar system) until the temporal stability of the calibration constant is verified. With several lidar systems we discovered both a day to day variance above the noise error, maybe caused by thermal influence on the detection electronics or optics, and long-term changes due to degradations of various components. The 90° difference can be achieved quite accurate by mechanical means (POLIS), but also using good actuators, as it is probably the case in David (APB 2012) because there no errors are mentioned for the measurement angles. The possible detector saturation at ±45° is an issue, but is solved by means of a polka-dot attenuator on top of the telescope, which doesn't influence the ratio of the polarization measurements. Such an attenuator would also be necessary at smaller angles, albeit with lower attenuation.

In Figures 6, 8, 10, 12, 13 and 14, could you improve the PDLR-graph so that the reader may see the data points? Why is the PLDR not retrieved below 2 and above 4 km? It may be useful for the reader. In the same way, in Figures 5, 7 and 9, could you modify the δv color scale? I only see two colors while a 8-bins color scale is used.

We changed Figures 6, 8, 10, 12 to show the retrieved PLDR below 2 km. Above 4 km the aerosol load is too low to calculate the PLDR with significant uncertainty. We removed Figure 13 as suggested by Reviewer #1.

In their assumed two-component mixture, S. Groß et al. use "for the aerosol type separation 0.30 at 532 nm for dust and 0.02 for marine aerosols according to the findings for pure Saharan dust and marine aerosols (Freudenthaler, 2009, Groß 2011b)". According to the observed variability in δp in the quoted papers, how is the 0.30 value chosen? Which value is used at 355 nm? To what extent do the corresponding uncertainties (at 355, 532 nm) modify your conclusions?

The chosen value represents the mean value of the measurements presented in the referenced literature. Certainly there is a natural variability of these values, however this variability was found to be smaller than our measurement uncertainties. Uncertainties of the used input values result in uncertainties of 10-30% of the retrieved quantities as stated in the referenced literature. As this comparison is performed for sun-photometer and lidar measurements at 500 nm and 532 nm, respectively, we do not use a value for 355 nm.

On the interpretation of the measurements
I disagree with the interpretation proposed by S. Groß et al. on several points.

1: To interpret their lidar measurements, S. Groß et al. assume a two-component particle mixture (page 19331, line 20). In the Caribbean, I would rather expect a three- component particle mixture, with water-soluble, sea-salt and dust particles to be more realistic: some back-trajectories (like the blueish) fall very close to sea level. While sea-salt particles can be found up to the tropopause (Ikegami 1994), could you discuss on your assumption of a two-component mixture? Reference literature to three-component particle mixtures (Sugimoto et al. Atm. Res.2010, David et al. ACP2013) are not quoted, while they may interest potential future readers. How do you discriminate non-spherical dust from sea-salt particles, which are non-spherical below 40 % relative humidity? This remark is important because aerosols are then classified at the end of the manuscript.

Our assumption of a two-component mixture in the lowermost layers is based on co-located in-situ measurements; Publications within this Special Issue are in preparation. The separation of sea-salt particles and dust was performed in the lowermost layers where the relative humidity was always larger 40 %.

2: As detailed in the introduction, reference literature exist showing that δp is modified for an aged Saharan dust plume (Wiegner et al. 2011) compared to values measured in fresh Saharan dust plumes (Groß et al. 2011b). Additionally, aerosol lifetime (Amiridis 2009) modifies the lidar ratio. However, in this manuscript, S. Groß et al. arrive to the opposite conclusion. How do you explain this difference? Is your conclusion a general established fact or a specific particular case? I do not understand the comparison of the SALTRACE experiment in the Caribbean with former experiments performed in Munich and during SAMUM campaigns a few years before. Could you assume that the source regions are the same, and if they are, that the activity of these sources is the same? On this point, I agree with Reviewer #1.

The work of Amiridis et al., 2009 deals with lidar measurements of biomass burning aerosols and is not suited for a comparison with our dust measurements here. In our analysis we found no significant differences in consequence of different activation methods or source regions. For the dust layers observed over Barbados and Munich (Wiegner et al., 2011) we found similar dust source regions.

3: I have some concerns with the classification proposed by S. Groß et al.

i) In the classification scheme, the plotted quantities (i.e. δp and Sp) are representative of the particles mixture and hence not specific to one type of particles (see Miffre et al. GRL2011 for the difference between δp and δns). δp is not a tracer for nonspherical particles (David et al., ACP2013). A "pure case" is however often reported in the manuscript (in the abstract and in the text). Could you provide evidence of a "pure case" here? Can we find "pure case" in the atmosphere? The coauthors have already used this terminology but it has never been defined in terms of chemistry and particles content. Optical devices are not sensitive enough to claim the existence of pure cases (one compound).

We do not see the point of this comment. The classification scheme shown in Figure 16 and adopted from other peer-reviewed publications is based on a multitude of co-located and synergistic lidar and in-situ measurements, while the stated article shows lidar measurements of a single event of volcanic ash and Saharan dust mixtures. Furthermore the stated paper declares 'Aerosol UV-depolarization serves as an independent means to discriminate ns from s-atmospheric particles' while in the next sentence of this comment they say 'δp is not a tracer for nonspherical particles (David et al., ACP2013)'. Our assumption of 'pure dust' is based on coordinated airborne in-situ measurements of the chemical and microphysical parameters of the observed aerosol layers. These results will be published in further publications within this Special Issue.

ii) Above all, though δp and Sp are intensive, a great variability can be observed in Sp and δp just by varying the size, the shape or the chemical composition. As published by M. Kahnert (JQSRT, 2015), a prerequisite for a potential classification scheme is that the variation in δp among particles in the same type is small compared to differences in δp among particles of different types and according to the state-of-the art literature, this is not a given. How do you account for this publication?

The publication of Kahnert deals with scattering of single particles in which case the shape and the chemical composition of the particle is of great importance. Lidar measurements represent measurements of a certain volume of air with a composition of different shape, chemical properties and orientation. From all our measurements including SAMUM, SALTRACE and long-range transported Saharan dust to Europe within EARLINET we do not see a strong variability in δp and Sp for Saharan dust plumes which had most properly no influence from other aerosol types. We do not know which state-of-the art literature is meant here showing that the intensive optical properties of one type varying stronger than the intense optical properties of different aerosol mixtures.

4: S. Groß et al. conclude that the intensive properties do not vary over several thousands of kilometers. Literature Reference (Ridley et al. ACP2013) indeed shows that the particle size distribution is modified during transport "Dust particle size showed a weak exponential relationship to dust age. Two cases of freshly uplifted dust showed quite different characteristics of size distribution". Following the link that exists between δp and the particles size, the particle depolarization is then modified. How do you account for this remark in regards to your conclusion that δp remains constant? By looking at Figure 14 in detail, a potential reader may wonder if this conclusion results from the atmosphere or from the lack of precision or/and sensitivity of the experiment. Could make some comment on this?

We guess that not the publication of Ridley et al. (GRL2013, ACP2014) but the publication by Ryder et al. (ACP2014) is meant in this comment. We totally agree that δp is dependent on the particles size. Following the results published by Ryder et al. the difference in δp for long-range transported dust in the Caribbean compared to fresh δp measurements close to the source should be in the range of 0.01 to 0.02. These are about the changes in δp we observed at Barbados and report in our article. Changes of the microphysical properties of long-range transported dust are under investigation and will be published in separate articles within this Special Issue. Referring to the comment on Figure 14 it is clear that the uncertainties in the retrieved optical properties are dependent on the measurement/aerosol conditions. Most of the measurement points shown in Figure 14 clearly show constant values with small uncertainties.

One specific comment

Page 19340, line 13: S. Groß et al. wrote that "It has been shown that the lidar ratio and the particle depolarization ratio are quite different for different types of aerosols" and quoted reference to Sakai et al. (2010) to justify this statement. In their paper, Sakaï et al. only addressed the particle depolarization and nothing is said about the lidar ratio. Could you provide another reference?

We added more references addressing particle depolarization and lidar ratio.

Interactive comment on “Characterization of long-range transported Saharan dust at the Caribbean by dual-wavelength depolarization Raman lidar measurements” by S. Groß et al.

PR Rairoux
Received and published: 8 September 2015

We thank Dr. Rairoux for his suggestions to help us improve the paper.

The answers are given in a direct response (bold, italic).

The task of describing particles optical properties after long range transport is a difficult task, as already quoted in the literature. The work presented by Gross et al. intends to reproduce such work concerning Sahara dust. However such event in the SALTRACE region of the Earth has never been reported before and it is very interesting to report how the optical properties of atmospheric aerosol are changing after crossing both the African continent and the Ocean. Because the methodology used to analyze with lidar device the change in aerosol optical properties after long-range transport is not new, it will be interesting for the readers that the authors quote others methodologies applied for such analysis as for example Sugimoto et al., AO 2006, Shimizu et al. JGR 2004 , David et al, ACP 2013. I have some concerns with this manuscript.

We followed the advice to include further references in the text.

1. The title does not refer the paper content. Gross et al. presented an analysis of a few cases, which is not a characterization that relies on the generalization of useful and well accepted physical, chemical or geophysical characteristics. Moreover, the study only relies on aerosol optical properties and not on aerosol chemical properties.

We agree and changed the title to ‘Optical properties of long-range transported Saharan dust over Barbados as measured by dual-wavelength depolarization Raman lidar measurements’

2. Why is the individual profile of the aerosols depolarization not shown in the PBL for the volume depolarization? It will strongly help the reader to improve the comprehension on how this parameter behaves in the atmosphere.

We changed the figures to show the particle linear depolarization ratio also in the PBL.

3. In the introduction, why is Earthcare program here quoted? It has nothing to do with the proposed analysis of the field campaign.

The basic lidar classification scheme of the future EarthCARE mission is mainly based on dust lidar measurements close to the source region. Up to now it was rather unclear if the thresholds derived from these measurements are also valid for long-range transported Saharan dust. As our measurements and analysis provide information on this topic we mention this in the introduction.

4. What do we learn that the PLDR, presented in figure 14 remains constant within the error bars? Same question with figure 15 on the Lidar ratio?

From Figure 14 and 15 we see that the optical properties (the particle depolarization ratio and the lidar ratio) do not show large differences for long-range transported Saharan dust compared to fresh dust close to the source regions. Possible modification of the particle microphysical and

chemical properties are either rather small or do not have significant influence on the derived optical properties. More information of the microphysical and chemical properties of long-range transported Saharan dust will be given in additional publications within this Special Issue (currently under preparation).

5. My main concern is relative to figure 16 and the way to use intensitive optical parameters (Lidar ratio and PLDR) to classify aerosol. It is a first tentative but it should not be considered as a general method. This because the sensitivity and the accuracy of the measurements are not high enough to realize this classification and only specific cases are shown on this 2D plot. The atmospheric content shows many examples of external mixed aerosol with the same PLDR and Lidar ratio values and different kind of particles with different microphysical properties. On this topic, can the authors discuss on what does "Pure Dust" mean and this quantitatively and not qualitatively.

Certainly aerosol typing of lidar measurements alone is more uncertain than in combination with other information. Furthermore it is crucial that the uncertainties of the derived optical properties are small enough to derive a significant result. Another problem is that mixtures of different aerosol types may result in the same optical properties. Here further information might be of some help. For the question about a quantitative discussion about 'Pure dust' we refer to a separate paper within this Special Issue concerning the chemical composition of the Saharan dust layer which is currently under preparation.

Summary
9/15/2015 4:55:33 PM

Differences exist between documents.

New Document:	**Old Document:**
SALTRACE-POLIS-rev	SALTRACE-POLIS
26 pages (9.56 MB)	25 pages (10.19 MB)
9/15/2015 4:55:27 PM	9/15/2015 4:55:26 PM
Used to display results.	

Get started: first change is on page 1.

No pages were deleted

How to read this report

Highlight indicates a change.
~~**Deleted**~~ indicates deleted content.
indicates pages were changed.
indicates pages were moved.

Manuscript prepared for Atmos. Chem. Phys.
with version 2015/04/24 7.83 Copernicus papers of the LaTeX class copernicus.cls.
Date: 15 September 2015

Optical properties of long-range transported Saharan dust over Barbados as measured by dual-wavelength depolarization Raman lidar measurements

Silke Groß[1], Volker Freudenthaler[2], Kerstin Schepanski[4], Carlos Toledano[3], Andreas Schäfler[1], Albert Ansmann[4], and Bernadett Weinzierl[1,2]

[1]Deutsches Zentrum für Luft- und Raumfahrt (DLR), Institut für Physik der Atmosphäre, Oberpfaffenhofen, Germany.
[2]Ludwig-Maximilians-Universität, Meteorologisches Institut, München, Germany
[3]Universitat de Valladolid, Spain.
[4]Leibniz-Institut für Troposphärenforschung (TROPOS), Leipzig, Germany.

Correspondence to: Silke Groß(silke.gross@dlr.de)

Abstract. Dual-wavelength Raman and depolarization lidar observations were performed during the Saharan Aerosol Long-range Transport and Aerosol-Cloud interaction Experiment at Barbados in June and July 2013 to characterize the optical properties and vertical distribution of long-range transported Saharan dust after transport across the Atlantic Ocean. Four major dust events were studied during the measurements from 15 June 2013 to 13 July 2013 with aerosol optical depths at 532 nm of up to 0.6. The vertical aerosol distribution was characterized by a three-layer structure consisting of the boundary layer, the entrainment or mixing layer, and the pure Saharan dust layer. The upper boundary of the pure dust layer reached up to 4.5 km height. The contribution of the pure dust layer was about half of the total aerosol optical depth at 532 nm. The total dust contribution was about 50-70% of the total aerosol optical depth at 532 nm. The lidar ratio within the pure dust layer was found to be wavelength independent with mean values of 53 ± 5 sr at 355 nm and 56 ± 7 sr at 532 nm. For the particle linear depolarization ratio wavelength independent mean values of 0.26 ± 0.03 at 355 nm and 0.27 ± 0.01 at 532 nm have been found.

1 Introduction

Aerosol particles play a key role in the Earth's climate system and affect the Earth's radiation budget in two different ways; directly by interacting with solar and terrestrial radiation (scattering and absorption) and indirectly by acting as cloud condensation nuclei and therewith influencing the clouds microphysical and optical properties and the clouds lifetime. Up to now the impact of aerosols on the global climate system is not fully understood (Forster and et al., 2007; Penner et al., 2011; Boucher et al., 2013). One main reason is the strong variability of aerosols. The sign and the magnitude of the radiative forcing crucially depends on the vertical distribution of aerosols, their microphysical properties and chemical composition, the reflectance of the underlying surface and the occurrence and amount of clouds (Forster and et al., 2007). However, knowledge of the temporal and vertical aerosol distribution on the global scale is limited (Penner and et al., 2001; IPCC, 2013). Additionally, significant sources of uncertainty result from deficits of satellite-based measurements in the determination of global mean AOD (Su et al., 2013), and from the insufficient knowledge of the impact of mixing, aging processes and transport on the aerosol optical and microphysical properties.

Advanced lidar systems like Raman lidar systems (Ansmann et al., 1990, 1992) or high spectral resolution lidar (HSRL) systems (Shipley et al., 1983; Shimizu et al., 1983; Piironen and Eloranta, 1994) with polarization sensitive channels (Sassen et al., 1989; Freudenthaler et al., 2009) provide information about the optical properties of aerosol layers. Spaceborne lidar measurements are an excellent tool to examine the global vertical distribution of aerosols. The Cloud-Aerosol Lidar with Orthogonal Polarization (CALIOP) on board the Cloud-Aerosol Lidar and Infrared Pathfinder Satellite Observations (CALIPSO) is an elastic backscatter lidar systems (Winker et al., 2009) and has only limited capability to distinguish different types of aerosols (Omar et al., 2009). In contrast, with the Cloud-Aerosol Transport System (CATS) currently flying on board the international space station (ISS) and the future ESA satellite mission EarthCARE polarization sensitive HSRL systems are deployed, having the potential to classify different aerosol types (Burton et al., 2012; Groß et al., 2013, 2015). However, current classification schemes for EarthCARE lidar measurements are mainly based on measurements of pure and fresh aerosol types (Groß et al., 2011a, 2014; Illingworth and et al., 2014). But as the optical properties are related to the microphysical properties like particle size, particle shape and chemical composition (Gasteiger et al., 2011b, a), aerosol aging, mixing and modification during transport can have an impact on the lidar derived optical properties, as well as on their wavelength dependence. For example, for measurements of the lidar ratio over Greece Amiridis et al. (2009) found that both, the value and the wavelength dependence of the lidar ratio of biomass burning aerosols may change with aerosol lifetime. Thus, possible changes of the lidar derived optical properties have to be investigated and considered for proper aerosol classification.

Mineral dust is a major component of the atmospheric aerosol (Haywood and Boucher, 2000; Forster and et al., 2007) with the Saharan desert being the most important source of mineral dust (Goudie and Middleton, 2001; Washington et al., 2003; Shao et al., 2011). Once lifted in the air, mineral dust can be transported over thousands of kilometers (Goudie and Middleton, 2001; Liu et al., 2008) exposed to the effects of aging and mixing. These effects change the optical, microphysical and cloud condensation properties. Coatings on mineral dust particles and mixing with other aerosols change the optical properties (Nousiainen, 2009; Redmond et al., 2010) and thus alter their radiative impact (Bauer et al., 2007). For example, biomass burning aerosols and mineral dust may become internally mixed when aging together (Hand et al., 2010) and thus change their size distribution, optical properties, hygroscopicity and their ability to act as cloud condensation nuclei (Wex et al., 2010). From measurements close to the dust source regions in comparisons to measurements in dust plumes over Cape Verde Weinzierl et al. (2011) found an indication of sedimentation of large particles in Saharan dust plumes during transport although sedimentation of large super-micron dust particles was less pronounced than expected from Stokes gravitational settling. Yang et al. (2013) assume a shape-induced particle sedimentation from measurements of transported dust with the space-based lidar system onboard the Cloud-Aerosol Lidar with Orthogonal Polarization (CALIOP) satellite mission (Winker et al., 2009). Wiegner et al. (2011) found an increase of the mean particle linear depolarization ratio at 355 nm of an aged Saharan dust plume over Central Europe compared to values measured in fresh Saharan dust plumes (Freudenthaler et al., 2009; Groß et al., 2011b). Up to now the mechanism and magnitude of dust aging is unknown, and whether and how it influences the optical properties of dust.

In this work we present dual-wavelength Raman and depolarization lidar measurements of long-range transported Saharan dust over Barbados. Our study includes a general investigation of aerosol layering and optical depth during our measurement period as well as the characterization of the Saharan dust layer and marine boundary layer by means of the lidar ratio and the particle linear depolarization ratio. These observations are crucial to investigate possible age-induced changes in the intensive lidar optical properties necessary for lidar based aerosol classification schemes. The measurements were performed during the SALTRACE closure experiment. A general description of the SALTRACE campaign, our lidar measurements and data analysis is given is Section 2. The results are presented in Section 3, and discussed in Section 4. Section 5 summarizes this work.

2 Measurements and Instrumentation

2.1 SALTRACE

In June and July 2013 the Saharan Aerosol Long-range Transport and Aerosol-Cloud interaction Experiment (SALTRACE, http://www.pa.op.dlr.de/saltrace/index.html) took place. SALTRACE was designed as a closure experiment combining ground-based lidar, in-situ and sun photometer instruments, with airborne aerosol and wind lidar measurements of the research aircraft Falcon of the Deutsches Zentrum für Luft- und Raumfahrt (DLR), satellite observations and model simulations. The main ground-site during SALTRACE was on Barbados where extensive lidar were performed. Barbados is an optimal location to characterize long-range transported dust after transport across the Atlantic Ocean. In addition, the 50-year Barbados dust record (Prospero et al., 1970) provides long-term information on year to year variability of trans-Atlantic dust transport to the Caribbean. The SALTRACE project continues the work started with the SAMUM-1 and SAMUM-2 (Ansmann et al., 2011) which aimed for characterizing Saharan mineral dust in the source regions and at different stages of dust lifetime. During SALTRACE particular focus was drawn on aerosol aging and mixing, and on aerosol removal processes. Therefore the physical, chemical and optical properties of the long-range transported Saharan dust layers were characterized in-depth to study the impact of long-range transported dust on the Earths radiation budget, clouds and precipitation. During SALTRACE, ground-based measurements at Barbados were performed at two main locations: ground-based in-situ measurements were made at the very eastern edge of the island at Ragged Point, whereas the lidar measurements were carried out at the Caribbean Institute of Meteorology and Hydrology (CIMH) at the south-western side of Barbados (13.14 N, 59.62 W). Sun photometer measurements were performed at both measurement sites. For this study we use the AERONET CIMEL (Holben et al., 1998) measurements 'Barbados_SALTRACE' performed at CIMH. SALTRACE measurements were carried out between 10 June and 15 July with the main closure experiments taking place between 20 June to 12 July 2013.

2.2 POLIS lidar system

In this work we present measurements of the small portable Raman and depolarization lidar system POLIS of the Meteorological Institute (MIM) of the Ludwig-Maximilians-Universität (LMU) München. POLIS is a 6-channel lidar system measuring the N_2-Raman shifted wavelengths at 387 nm and 607 nm and the elastic backscattered signals (cross- and parallel-polarized) at 355 nm and 532 nm (Freudenthaler et al., 2015). Thus profiles of the particle extinction coefficient α_p and backscatter coefficient β_p, of the lidar ratio S_p, and of the volume and particle linear depolarization ratio δ_v and δ_p at 355 nm and 532 nm can be retrieved. The full overlap of POLIS is at about 200 m to 250 m depending on system settings. The range resolution of the raw data is 3.75 m; the temporal resolution is 5-10 s depending on atmospheric conditions. The repetition rate of the frequently doubled and tripled Nd:YAG laser is 10 Hz with a pulse energy of 50 mJ at 355 nm and 27 mJ at 532 nm.

2.3 Data analysis

The particle extinction coefficient α_p is retrieved from the Raman signals at 387 nm and 607 nm (Ansmann et al., 1990), the particle backscatter coefficient β_p is derived from combined Raman and elastically backscattered lidar returns at 355/387 and 532/607 nm (Ansmann et al., 1992). The height dependent lidar ratio S_p=α_p/β_p can be derived from the ratio of both properties. Due to the low signal-to-noise ratio of the Raman channels during daytime, these measurements were restricted to night-time only. Furthermore, typical temporal averaging of one hour is necessary for analyzing α_p and S_p to achieve a sufficient signal-to-noise ratio. The temporal stability of the atmosphere within this time period has been validated by assessing the temporal evolution of the range corrected signal Pr^2 over the whole smoothing period. A typical vertical smoothing of ≈900 m (250 rangebins) is applied to further increase the signal-to-noise ratio. The errors of the retrieved optical properties are calculated according to Groß et al. (2011c).

From the co- and cross-polarized elastically backscattered signals the volume linear depolarization ratio δ_v and the particle linear depolarization ratio δ_p (Biele et al., 2000; Freudenthaler et al., 2009) are derived. The relative calibration factor of both polarization channels was determined with the $\pm45°$-calibration method (Freudenthaler et al., 2009) by manually rotating the receiver optics behind the telescope. Although the signal-to-noise ratio of the elastic channels is much better than for the Raman channels the same temporal average was used for the analysis of the nighttime Raman and depolarization measurements to get comparable results. The vertical average of the elastic signals is typically ≈550 m (150 rangebins), otherwise the vertical smoothing length is specified in the text. Details of the depolarization calibration and system performance can be found by Freudenthaler et al. (2009, 2015). The error calculation of δ_v and δ_p was done analogue to Freudenthaler et al. (2009).

To determine the dust contribution within the boundary layer and the intermediate layer, we determined the profile of the dust backscatter coefficient applying a procedure based on the work of Shimizu et al. (2004) and described by Tesche et al. (2009a) and Groß et al. (2011a) assuming a two-type mixture of dust and marine aerosols (based on coordinated in-situ measurements). The linear depolarization ratios used as input for the aerosol type separation are set to δ_d = 0.30 at 532 nm for dust and δ_{nd} = 0.02 for marine aerosols (relative humidity ≥40%) according to the findings for pure Saharan dust and marine aerosols (Freudenthaler et al., 2009; Groß et al., 2011b). The dust extinction coefficient is derived following the equation α_d=β_d*S_d. The lidar ratio of dust (S_d = 55 sr) is taken from Tesche et al. (2009b) and is in good agreement with the mean S_p-values we find for long-range transported Saharan dust during SALTRACE.

2.4 Dust source regions and transport

To identify dust source regions and transport way and time, we use a combination of backtrajectorie calculation and satellite observations. The trajectories were calculated with the Hybrid Single Particle Lagrangian Integrated Trajectory (HYSPLIT) model (Draxler and Rolph, 2012) and the NCEP Global Data Assimilation System (GDAS) meteorological data. Start time and height of the trajectories were chosen according to the analyzed lidar measurement time periods and the height ranges of the presumed dust layer. The duration of all backward trajectories is 312 hours. Different dust source activity over North Africa and thus different source region contributing to the dust plume observed at Barbados are identified from infra-red (IR) dust index images calculated from Meteosat Second Generation (MSG) Spinning Enhanced Visible and Infra-Red Imager (SEVIRI) observations (Figure 4). As described in detail in Schepanski et al. (2007), active dust sources are identified and recorded on a 1°x1° map covering Africa north of 10° N.

3 Results

3.1 General overview

During SALTRACE we observed a sequence of dust events with Saharan air masses being transported with easterly winds over the Atlantic to Barbados. The dust episodes often lasted several for days and provided, apart from shallow cumulus clouds, optimal measurement conditions in the dry and aerosol rich air. The dust events were interrupted by wet periods with strong convective activity and precipitation. Here we focus on the analysis of four major dust events.

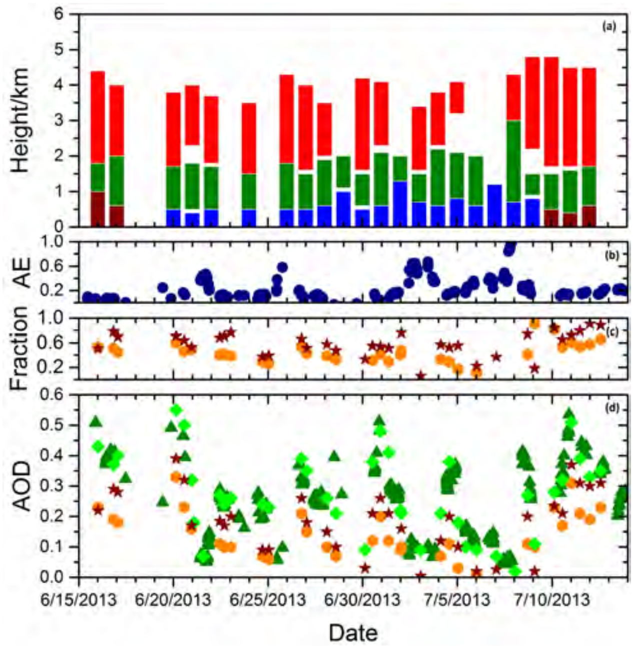

Figure 1. Time series of (a) aerosol layering during SALTRACE derived from POLIS lidar measurements during the evening measurement sessions, (b) Angström exponents between 440 nm and 870 nm (blue dots) from CIMEL sun-photometer measurements, (c) the fraction of pure dust optical depth (orange) and total dust optical depth (brown stars) to the total AOD, and (d) aerosol optical depth (AOD) at 500 nm derived from CIMEL sun-photometer measurements (dark green) and at 532 nm derived from POLIS lidar measurements (light green) and optical depth of the pure dust layer (orange) and of the whole dust contribution in the atmospheric column (brown stars) at 532 nm derived from POLIS lidar measurement.

The aerosol optical depth (AOD) at 500 nm and 532 nm during these major dust events reached values of up to 0.55. The corresponding Angström Exponent (AE) between 440 nm and 870 nm showed very low values of 0.2 and lower. The overall aerosol situation was characterized by a three layer structure (Figure 1). The optical properties of the boundary layer (up to 0.5 to 1.0 km) were mostly dominated by marine aerosols, except during the first and last measurement days. At heights from about 1.0 to 2.0 km the aerosol layer was composed of a mixture of predominantly dust and marine aerosols. This layer showed high variability with respect to aerosol load and mixture. During SALTRACE almost all cloud processes in the lower troposphere took place within this layer. Above this intermediate layer a Saharan dust layer was present almost permanently during our measurement period, except on 8th and 9th July when Tropical Storm 'Chantal' dominated the weather situation. During the main Saharan dust events this uppermost dust layer showed AOD values of about 0.2 at 532 nm, in some cases the AOD at 532 nm even reached values of more than 0.3. The contribution of this pure Saharan dust layer to the total AOD at 532 nm usually ranged between 30% and 60%, in some cases up to 80%. The total contribution of Saharan dust to the total AOD at 532 nm was 50-80%, except during Tropical Storm Chantal, when the Saharan dust contribution to the total AOD at 532 nm was only 20%. An overview over the vertical layering and the AOD is given in Figure 1.

3.2 Case Studies

We present four case studies, which are representative for the four dust events that occurred during the core period of SALTRACE. The date and time of the chosen cases studies are 20 June (23-24 UTC), 27 June (0-2 UTC), 1 July (7-9 UTC), and 11 July 2013 (23-24 UTC). One main topic of our analysis is to investigate whether the different dust events show a variability in the retrieved optical properties. Figure 2 shows a back-trajectory analysis for the four selected case studies. All trajectories show an advection from easterly directions and source regions located inside the Sahara region. However, the specific flow patterns of the air masses of the different events are quite different as well as possible source regions within the Saharan desert.

For the four case studies (20 June, 27 June, 1 July, 11 July 2013), different dust sources regions are found to be active (Figure 3). A brief overview on the dust contributing source regions and the meteorological regime resulting into dust uplift will be given in the following. HYSPLIT back-trajectories are analyzed to identify the dates on which the Saharan air mass observed over Barbados where likely over dust source regions over North Africa. For the first two cases (20 and 27 June), dust source activation over North Africa was dominated by the Harmattan flow (a dry and dusty trade wind over West Africa). The latter two July-cases (1 and 11 July) show an increase in deep convective activity and Haboobs (heavy dust storm) become a more frequent dust uplift mechanism compared to the June-cases.

3.2.1 20 June 2013; 23:30 – 24:00 UTC

Already during the first measurement period of the SALTRACE campaign we were able to observe a strong Saharan dust event with total AOD of up to 0.55. Dust sources contributing to the dusty air mass reaching Barbados on 20 June 2013 were active during 11 to 13 June 2013. On 11 June 2013, strong Harmattan winds and embedded nocturnal low-level jet (LLJ) forced dust uplift over the Adra and southeastern Hoggar region (NE Mali and SW Algeria). Entrained into the northeasterly Harmattan flow, dusty air is transported towards the tropical North Atlantic. On 12 June 2013, dust

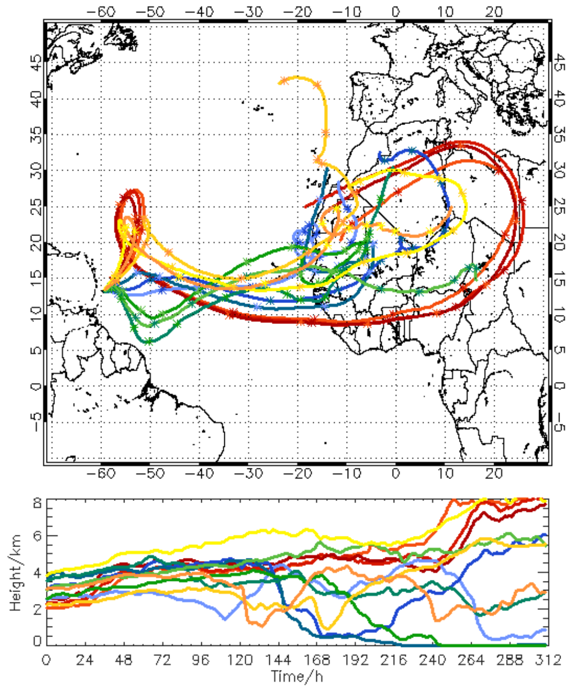

Figure 2. 312-h backward trajectories calculated with the Hybrid Single Particle Lagrangian Integrated Trajectory (HYSPLIT) model (Draxler and Rolph, 2012) and GDAS meteorological data for the pure dust layers on 20 June 2013, 23 UTC (reddish), 27 June 2013, 01 UTC (blueish), 1 July 2013, 8 UTC (greenish), and 11 July, 23 UTC (yellowish). The stars along the trajectories indicate 24-h time steps. The height range of the pure dust layers is indicated in Table 1.

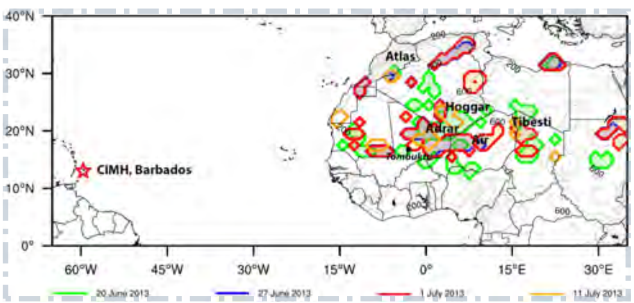

Figure 3. Active dust sources relevant for the four investigated case studies. The colors indicate which source region contributed to which dust event observed at Barbados.

emitted by strong Harmattan winds from the Niger flood plains south of Timbuktu (Mali) were uptaken by an air mass crossing the Atlantic and reaching Barbados on 20 June 2013.

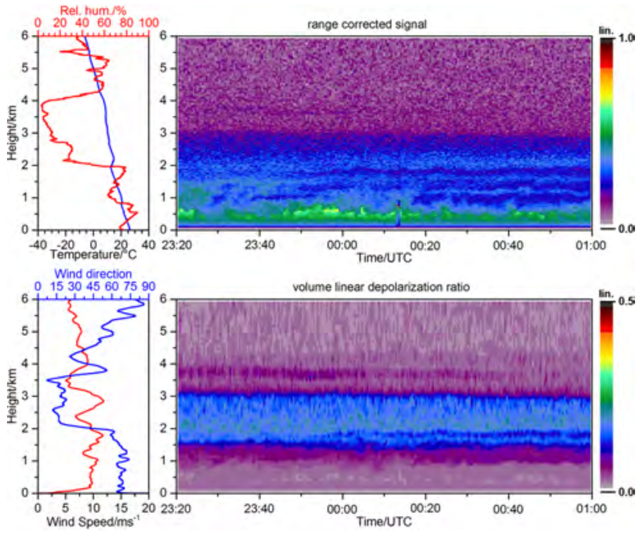

Figure 4. Radiosonde measurements of temperature and relative humidity (upper left panel) and of wind speed and wind direction (lower left panel), and lidar measurements of the range corrected signal (upper right panel) and of the volume linear depolarization ratio (lower right panel) at 532 nm between 20 June 2013, 23:00 UTC and 21 June 2013, 1 UTC. The radiosonde was launched on 21 June at 1:54 UTC

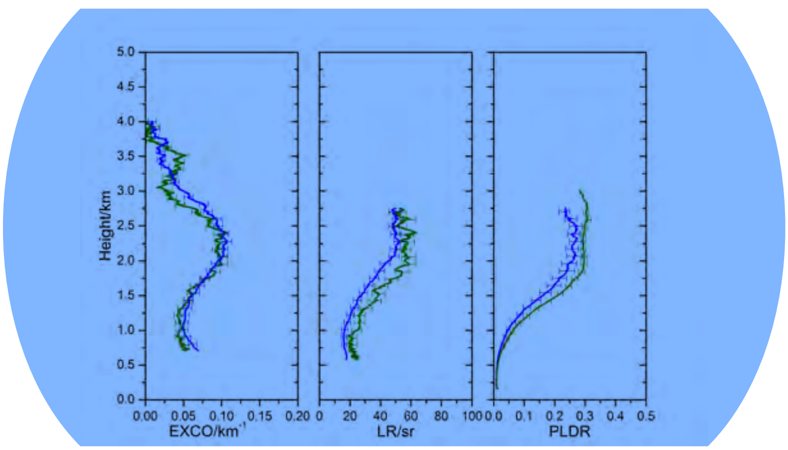

Figure 5. Profiles of the particle extinction coefficient (EXCO) and the lidar ratio (LR), and of the particle linear depolarization ratio (PLDR) of the pure dust layer at 355 nm (blue) and 532 nm (green) on 20 June 2013, 23:30 – 24:00 UTC. The error bars indicate the systematic errors.

Figure 4 gives an overview of the measurement situation in the night from 20 June to 21 June 2013 when the Saharan dust layer slowly faded away. The Saharan dust layer can be clearly identified by enhanced δ_v of about 0.15 in heights from 1.5 to 3 km. A clear signature to distinguish the dust layer from the mixing layer at about 0.8-1.5 km with rather similar values of the range corrected signal but lower δ_v values. In the lowermost 0.8 km the range corrected signal shows high values with low δ_v, which is an indication for a marine dominated boundary layer. In the height level of the Saharan Air Layer (SAL), the relative humidity is low (notice that lidar measurements and radiosonde measurements have an offset of about 2 hours in this case study) and the air masses were transported from mainly north-easterly directions. In the lowermost height level the relative humidity shows values between 60-80%. For the analysis of the vertical distribution of the extinction coefficient, the lidar ratio and the particle linear depolarization ratio (Figure 5) we use a time period between 23:30 – 24:00 UTC with very homogeneous conditions. Increased values of α_p are found up to 4 km, but highest α_p-values are found between 1.5 and 3.0 km with max. α_p of about 0.12 km^{-1}. Mean S_p-values in the dust layer are 56 $\pm$ 5 sr at 532 nm and 50 $\pm$ 4 sr at 355 nm. In the marine boundary layer mean S_p-values of 21 $\pm$ 3 sr at 532 nm, and 17 $\pm$ 2 sr at 355 nm are found with corresponding wavelength independent mean δ_p-values of $\approx$0.02. In the dust layer δ_p shows a slight wavelength dependence with mean values of 0.3 at 532 nm and 0.26 at 355 nm.

3.2.2 27 June 2013; 00:00 – 02:00 UTC

Air masses being over the North African continent at boundary layer heights (up to 3-5 km) and thus able to uptake dust during 20 to 22 June 2013 are likely to contribute to the dust layer observed over Barbados on 27 June 2013. On 20 June, dust source embedded in desert valleys scattered over the three mountain regions Hoggar, Aïr and Adrar were activated during the morning hours by nocturnal LLJs embedded in the Harmattan flow. The dusty air mass slowly propagated westward. On 21 June 2013, further dust emitted from dust sources over the Adrar Mountains (East Mali) and Southeast Mauritania was contributing.

Figure 6 gives an overview of the night-time measurements situation on 27 June 2013 over Barbados. The total AOD at 532 nm was as high as 0.4. The range corrected signal shows aerosol signature up to about 4 km, whereas the highest signals are observed in the lowermost aerosol layer up to about 0.6 km. δ_v shows high values of 0.15 in the height range between 1.5 km and 4 km clearly identifying the SAL. As observed during the case study of 20 June (23:30 – 24:00 UTC) the relative humidity in the SAL is low with values <40% and the temperature profile shows a weak inversion at the lower edge of the SAL. The dusty air masses arrived from mainly easterly directions. Within the SAL α_p was about 0.08 km^{-1} and decreased at heights above $\approx$3.5 km. S_p in the SAL shows mean values of 56 $\pm$ 5 sr at 532 nm and 55 $\pm$ 7 sr at 355 nm, the corresponding δ_p shows wavelength independent values of 0.26 $\pm$ 0.01 at 532 nm and 0.26 $\pm$ 0.03 at 355 nm (Figure 7). Within the boundary layer mean S_p-values of 21 $\pm$ 3 sr at 532 nm and 17 $\pm$ 2 sr at 355 nm are observed. The mean δ_p-values in the boundary layer are 0.06 $\pm$ 0.01 at 532 nm and 0.04 $\pm$ 0.01 at 355 nm.

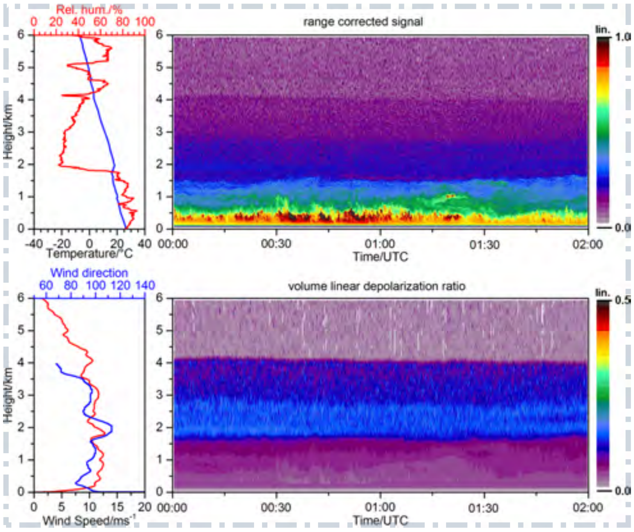

Figure 6. Same as Figure 4 but for 27 June 2013, 00:00 – 02:00 UTC. The radiosonde was launched on 27 June at 0:24 UTC.

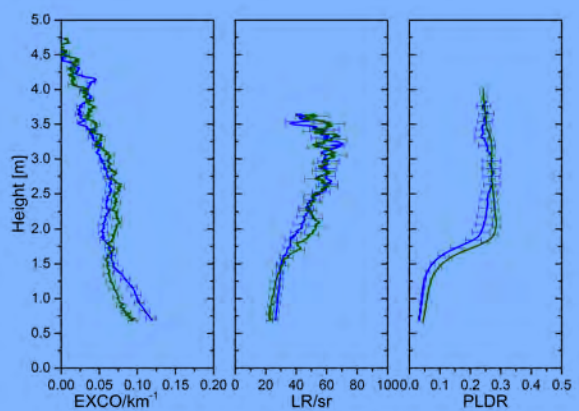

Figure 7. Same as Figure 5 but for 27 June 2013, 00:00 – 02:00 UTC.

3.2.3 1 July 2013; 07:00 – 08:45 UTC

On 1 July a total AOD of about 0.55 was observed over Barbados. Back-trajectories show that Saharan air masses arriving Barbados on 1 July 2013 remained over West Africa for quite some time during the 19 and 25 June before entering the tropical North Atlantic. During these days, frequently active dust source regions were located embedded in the desert valley of the Adra Mountains, but also in central Mali where sand sheets and ancient drainage systems characterize the landscape. Dust sources were activated by both, nocturnal LLJ embedded in the Harmattan flow resulting to morning on-set of dust emission and dust fronts (Haboobs) related to downdrafts generated by MCSs (Meso-scale Convective System) during the late afternoon and night.

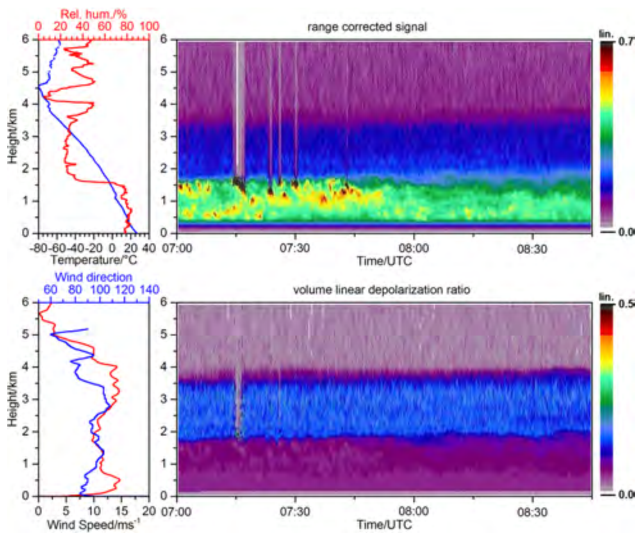

Figure 8. Same as Figure 4 but for 1 July 2013, 07:00 – 08:45 UTC. The radiosonde was launched on 1 July at 00 UTC.

The measurement situation on 1 July (7:00-9:45 UTC) was similar to those during the prior events (Figure 8). Within the SAL, characterized by δ_v-values of about 0.15, the relative humidity is < 40%, whereas the boundary layer shows large RH-values of up to 80%. The wind direction within the aerosol layers was mainly easterly. Inside the SAL α_p values of about 0.75 km^{-1} are observed (Firuge 9). In the boundary layer α_p increases to values of about 0.13 km^{-1}. S_p in the dust layer is wavelength independent with mean values of 54 $\pm$ 7 sr at 532 nm and 53 $\pm$ 6 sr at 355 nm. δ_p shows mean values of 0.27 at both wavelengths. In the boundary layer mean S_p-values of 30 $\pm$ 4 sr at 532 nm and 25 $\pm$ 2 sr at 355 nm are found. Mean δ_p-values are 0.06 $\pm$ 0.01 at 532 nm and 0.04 $\pm$ 0.01 at 355 nm.

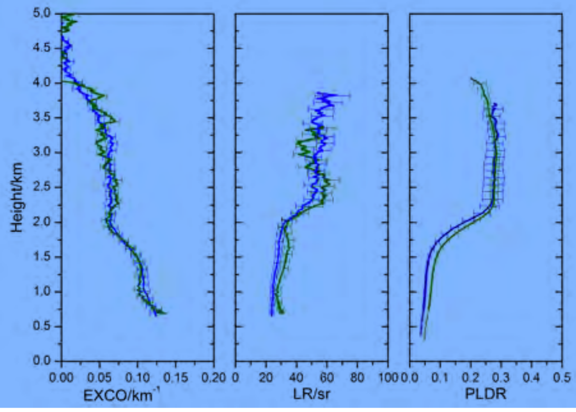

Figure 9. Same as Figure 5 but for 1 July 2013, 07:00 – 08:45 UTC.

3.2.4 11 July 2013; 23:00 – 24:00 UTC

The last dust event we observed during SALTRACE started after the passage of Tropical Storm 'Chantal' on 9 July 2013 and lasted until the end of our measurements on 12 July 2013. Highest dust AOD up to 0.4 was observed on 11 July. Compared to the previous cases, the atmospheric humidity over North Africa has increased and deep convective clouds form in particular over orographic regions over the Sahara. The convective clouds grow to MCS, which generate Haboobs in particular over West Africa. Contributing dust originating from source over the southwest flanks of the Hoggar Massif were emitted by in the Harmattan flow embedded LLJs.

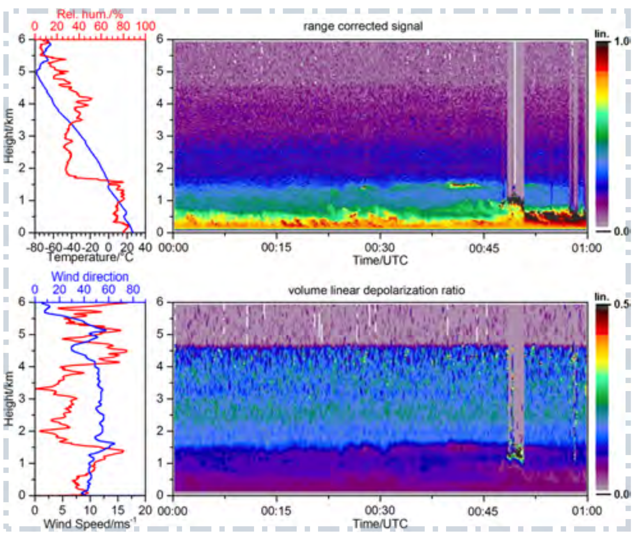

Figure 10. Same as Figure 4 but for 11 July 2013, 23:00 – 24:00 UTC. The radiosonde was launched on 11 July at 23:26 UTC.

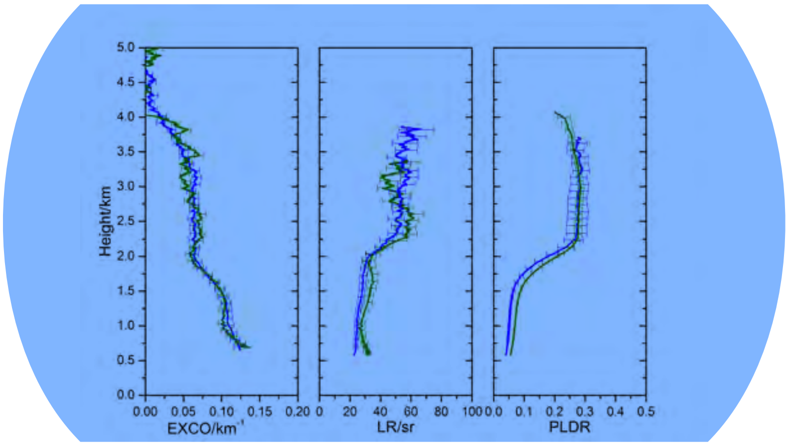

Figure 11. Same as Figure 5 but for 11 July 2013, 23:00 – 24:00 UTC.

The top of the SAL observed over Barbados was at about 4.8 km height. Figure 10 gives an overview of the night measurements from 10 July to 11 July (0 – 1 UTC). High intensity of the range corrected signal was found in the boundary layer below about 0.5 km. The lowest signal intensity was found above about 3.0 km. However δ_v-values of 0.15–0.18 clearly identify the dust layer from 1.5 up to about 4.8 km. The air masses arrived from north-easterly directions, and the SAL is characterized by very low wind speed (except for the uppermost 0.5 km). Within the SAL the relative humidity shows again low values of <40% while it jumps to values of about 80% in the boundary layer. α_p is about 0.1 wavelength independent in the SAL and shows even slightly higher values in the lowermost 1.5 km (Figure 11). Mean S_p values of 56 $\pm$ 4 sr at 532 nm an 50 $\pm$ 4 sr at 355 nm are found in the SAL with wavelength independent δ_p of 0.27 $\pm$ 0.01 and 0.26 $\pm$ 0.02 at 532 nm and 355 nm. In the boundary layer we find wavelength independent mean S_p-values of 35 sr with corresponding δ_p of 0.1 $\pm$ 0.01 at 532 nm and 0.14 $\pm$ 0.01 at 355 nm, indicating a certain amount of dust mixed into the boundary layer.

The main findings of the four case studies are summarized in Table 1.

3.3 General findings

The mean values of S_p and δ_p within the SAL and within the boundary layer are summarized in Table 2. The mean S_p values in the SAL range between 49 sr and 60 sr at 532 nm and between 47 sr and 63 sr at 355 nm. The overall mean S_p-values for long-range transported Saharan dust, considering all analyzed data, are 56 $\pm$ 7 sr and 53 $\pm$ 5 sr at 532 nm and 355 nm. δ_p-values in the SAL range between 0.26 and 0.3 at 532 nm and between 0.24 and 0.29 at 355 nm. The overall mean δ_p-values are of 0.27 $\pm$ 0.01 at 532 nm and 0.26 $\pm$ 0.03 at 355 nm. However, during the first Saharan dust event δ_p shows a slight but significant wavelength dependence with layer mean values of δ_p = 0.3 $\pm$ 0.01 at 532 nm and δ_p = 0.26 $\pm$ 0.02 at 355 nm. Analysis of the remaining SALTRACE

Table 1. Layer mean values for the case studies of lidar ratio S_p and particle linear depolarization ratio δ_p including systematic errors ($\pm$), the standard deviations of the values within the height range (σ) indicating the variability of the values within the layer, and the retrieved type of aerosol for the each lidar system and wavelength.

Height a.g.l./km	Lidar ratio / sr	PLDR	Layer
20 June 2013; (23–23:30 UTC)			
0.25**/0.5* – 1.5	21 ± 3 (σ = 1) (532 nm)*	0.02 ± 0.01 (σ = 0.01) (532 nm)**	Boundary layer
	17 ± 2 (σ = 1) (355 nm)*	0.02 ± 0.01 (σ = 0.01) (355 nm)**	
2.0 – 2.5	56 ± 5 (σ = 2) (532 nm)	0.30 ± 0.01 (σ = 0.01) (532 nm)	Dust layer
	50 ± 4 (σ = 2) (355 nm)	0.26 ± 0.02 (σ = 0.01) (355 nm)	
27 June 2013; (00–02 UTC)			
0.25**/0.5* – 1.5	25 ± 3 (σ = 1) (532 nm)*	0.06 ± 0.01 (σ = 0.01) (532 nm)**	Boundary layer
	28 ± 2 (σ = 1) (355 nm)*	0.04 ± 0.01 (σ = 0.01) (355 nm)**	
2.0 – 3.5*/3.75**	56 ± 8 (σ = 5) (532 nm)*	0.26 ± 0.01 (σ = 0.01) (532 nm)**	Dust layer
	55 ± 7 (σ = 7) (355 nm)*	0.26 ± 0.03 (σ = 0.01) (355 nm)**	
01 July 2013; (07–09 UTC)			
0.4**/0.5* – 1.5	30 ± 4 (σ = 2) (532 nm)*	0.06 ± 0.01 (σ = 0.01) (532 nm)**	Boundary layer
	25 ± 2 (σ = 1) (355 nm)*	0.04 ± 0.01 (σ = 0.01) (355 nm)**	
2.25 – 3.5*/3.75**	54 ± 7 (σ = 8) (532 nm)*	0.27 ± 0.01 (σ = 0.01) (532 nm)**	Dust layer
	53 ± 6 (σ = 3) (355 nm)*	0.27 ± 0.03 (σ = 0.01) (355 nm)*	
11 July 2013; (23–24 UTC)			
0.4**/0.75* – 1.5	35 ± 3 (σ = 2) (532 nm)*	0.10 ± 0.01 (σ = 0.02) (532 nm)**	Boundary layer
	35 ± 2 (σ = 1) (355 nm)*	0.14 ± 0.01 (σ = 0.02) (355 nm)**	
2.0 – 4.0	56 ± 7 (σ = 6) (532 nm)	0.27 ± 0.01 (σ = 0.01) (532 nm)	Dust layer
	50 ± 4 (σ = 6) (355 nm)	0.26 ± 0.02 (σ = 0.01) (355 nm)	

measurements show comparatively lower mean values at 532 nm with almost constant mean values at 355 nm.

The boundary layer during SALTRACE was dominated by marine aerosols, with a contribution of dust in various amounts of dust, especially during the last observed Saharan dust event. The mean S_p–values range between 21 sr and 36 sr at 532 nm and between 16 sr and 35 sr at 355 nm. The overall mean S_p shows a wavelength independent value of 26 sr. Highest S_p values are found during the last observed dust event, indicating an increased amount of dust mixed into the boundary layer. This is in good agreement with the mean δ_p-values of >0.1 in the boundary layer during the last observed dust event, clearly identifying dust mixed in the boundary layer (Tesche et al., 2009b; Groß et al., 2011a). During days when marine aerosols were the dominant type in the boundary layer

δ_p is low with mean values between 0.01 and 0.04 at both wavelengths. The overall mean δ_p-values are δ_p = 0.05 ± 0.01 at 532 nm and δ_p = 0.04 ± 0.01 at 355 nm.

4 Discussion

4.1 Comparison to former dust measurements

The lidar measurements performed at Barbados during SALTRACE and presented in this work give us the opportunity to compare the intensive lidar properties (e.g. the lidar ratio and the particle linear depolarization ratio) of Saharan dust derived close to the source region in Quarzazate, Morocco, during SAMUM-1 (Freudenthaler et al., 2009) with measurements of mid-range transported Saharan dust at Cape Verde during SAMUM-2 (Groß et al., 2011b) and of long-range transported Saharan dust over the Atlantic Ocean. From these studies possible changes due to transport and aging can be studied. Comparisons with measurements of long-range transported Saharan dust over Central Europe (Wiegner et al., 2011) furthermore enable to investigate whether not only the transport time but also the transport path has an effect of particle aging.

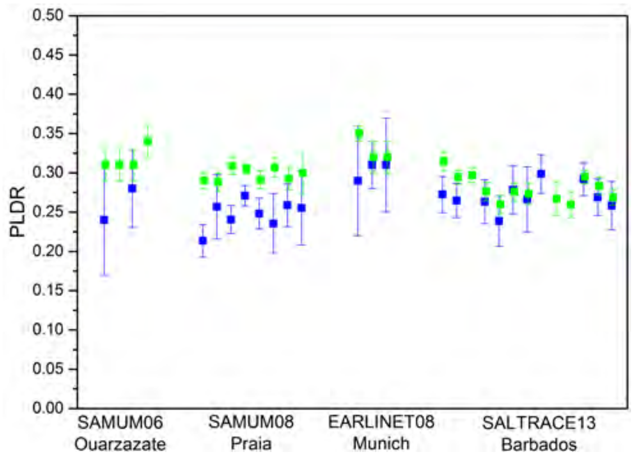

Figure 12. Mean values of the particle linear depolarization ratio of Saharan dust at 355 nm (blue) and 532 nm (green) derived for fresh Saharan dust on 4 days during SAMUM-1 in Ouarzazate, Morocco in 2006 (SAMUM06) (Freudenthaler et al., 2009), for mid-range transported Saharan dust on 8 days during SAMUM-2 at Cape Verde in 2008 (SAMUM08) (Groß et al., 2011b), for long-range transported dust over Central Europe on 3 days at Munich, Germany in 2008 (EARLINET08) (Wiegner et al., 2011), and for long-range transported Saharan dust over the Caribbean on 13 days during SALTRACE at Barbados in 2013 (SALTRACE13). The error bars denote the systematic errors.

An overview of δ_p measurements at 355 nm and 532 nm is given in Figure 12. For each measurement campaign a number of days (4, 8, 3, 13) is included in this study. The main findings are: δ_p and its wavelength dependence does not change for measurements of fresh Saharan dust at Morocco, close to the source regions, and for dust mid-range transported at Cape Verde. The wavelength dependent overall mean values are 0.31 ± 0.01 (532 nm) and 0.25 ± 0.07 (355 nm) for fresh Saharan dust (Freudenthaler et al., 2009) and 0.3 ± 0.01 (532 nm) and 0.25 ± 0.03 (355 nm) for mid-range transported Saharan dust (Groß et al., 2011b). For long-range transported Saharan dust towards Central Europe we found slightly higher values of 0.34 ± 0.02 and 0.30 ± 0.05 at 532nm and 355 nm, respectively (Wiegner et al., 2011). At Barbados we find a slightly lower mean δ_p-value of 0.27 ± 0.01 at 532 nm and a rather constant mean value of 0.26 ± 0.03 at 355 nm. The observed differences between δ_p for long-range transported dust compared to the values for pure and mid-range transproted dust are small. However, we see different alterations of the optical properties for long-range transported Saharan dust towards Central Europe and of long-range transported Saharan dust over the Atlantic Ocean towards the Caribbean. We do not longer see a wavelength dependence for δ_p at 355 nm and 532 nm for long-range transported Saharan dust towards the Caribbean within the uncertainty range. The differences of δ_p for long-range transported Saharan dust over Central Europe and over Barbados lead to the assumption that not only the time of long-range transport, but also the transport path, and the conditions during transport may be of importance when investigating the effects of aging and transport. This assumptions will be subject of further studies.

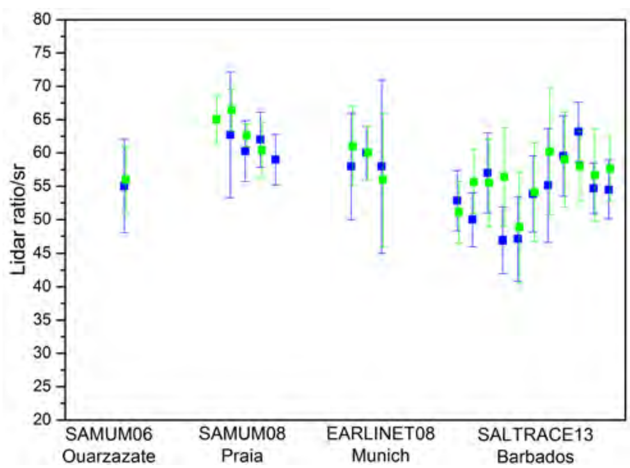

Figure 13. Mean values of the lidar ratio of Saharan dust at 355 nm (blue) and 532 nm (green) derived for fresh Saharan dust (mean campaign value) during SAMUM-1 in Ouarzazate, Morocco in 2006 (SAMUM06) (Tesche et al., 2009b), for mid-range transported Saharan dust on 5 days during SAMUM-2 at Cape Verde in 2008 (SAMUM08) (Groß et al., 2011b), for long-range transported dust over Central Europe on 3 days at Munich, Germany in 2008 (EARLINET08) (Wiegner et al., 2011), and for long-range transported Saharan dust over the Caribbean on 10 days during SALTRACE at Barbados in 2013 (SALTRACE13). The error bars denote the systematic errors.

A similar analysis was performed for S_p measurements during SAMUM-1 (mean value), SAMUM-2 (5 cases), the Munich event in 2008 (3 cases) and during the SALTRACE campaign (10 cases) (see

Table 2. Layer mean values of the lidar ratio S_p and particle linear depolarization ratio δ_p including systematic errors ($\pm$) of Saharan dust observations during SAMUM-1 in Morocco close to the source regions (Freudenthaler et al., 2009; Tesche et al., 2009b), of mid-range transported Saharan dust during SAMUM-2 at Cape Verde (Groß et al., 2011b), of long-range transported Saharan dust to Central Europe in Munich, Germany (Wiegner et al., 2011), and of long-range transported Saharan dust across the Atlantic Ocean at Barbados during SALTRACE.

Campaign	Lidar ratio / sr	PLDR	WL / nm
SAMUM-1	56 ± 5	0.31 ± 0.01	532
	55 ± 7	0.25 ± 0.07	355
SAMUM-2	62 ± 5	0.30 ± 0.01	532
	58 ± 7	0.25 ± 0.03	355
Munich	59 ± 7	0.34 ± 0.02	532
	59 ± 8	0.30 ± 0.05	355
SALTRACE	56 ± 7	0.27 ± 0.01	532
	53 ± 5	0.26 ± 0.03	355

Figure 13). For the fresh Saharan dust in Ouazazate wavelength-independent mean values of S_p=55 $\pm$ 7 sr at 355 nm and S_p=56 $\pm$ 5 sr at 532 nm were found (Tesche et al., 2009b). Slightly but not significantly higher lidar ratios were found during the Munich dust event and SAMUM-2 campaign for mid-range transported dust with wavelength-independent mean values of about 60 sr (Wiegner et al., 2011; Groß et al., 2011b). These slightly higher values are in good agreement with the study of Schuster et al. (2012) investigating lidar ratios of mineral dust for different regions over Northern Africa and finding the highest mean values for Saharan dust at Cape Verde. During SALTRACE the lidar ratios range between 47 sr and 63 sr with mean values of S_p = 56 $\pm$ 7 sr at 532 nm and S_p = 53 $\pm$ 5 sr at 355 nm. Altogether no significant changes in the lidar ratio can be found within the error bars for the fresh and the transported Saharan dust cases.

The mean values and mean uncertainties of S_p and δ_p for the different dust measurements are summarized in Table 2.

4.2 Impact on aerosol classification

It has been shown that the lidar ratio and the particle linear depolarization ratio are quite different for different types of aerosol (Cattrall et al., 2005; Müller et al., 2007; Sakai et al., 2010; Burton et al., 2012). Therefore aerosol classification schemes both at 355 nm and 532 nm have been developed based on these intensive lidar optical properties (Groß et al., 2011b; Burton et al., 2012; Groß et al., 2013; Illingworth and et al., 2014). Up to now those classification schemes do not sufficiently account for the effect of aerosol aging on the thresholds for the discrimination of the different aerosol types. With our measurements during the SALTRACE campaign, in combination with the findings of former measurements of fresh and mid-range transported dust during the SAMUM project and long-range transported dust measurements over Central Europe, we are now able to investigate the effect of transport and aging on the lidar optical properties of Saharan dust.

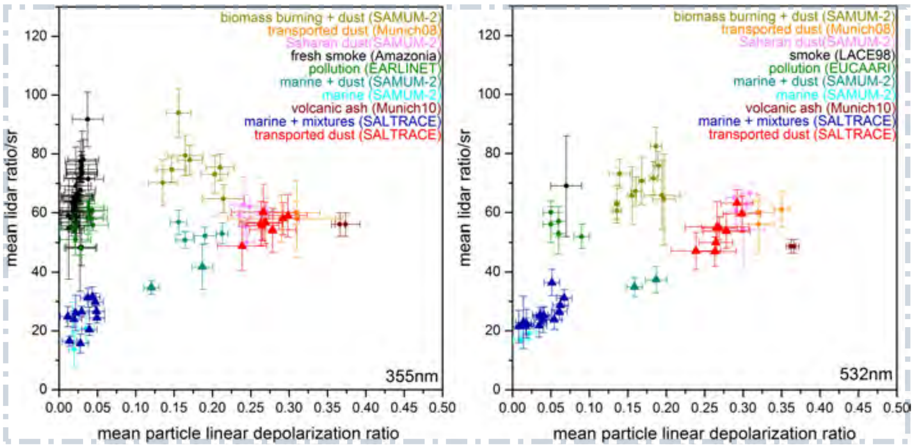

Figure 14. Aerosol classification at 355 nm (left) and 532 nm (right) based on the lidar ratio and the particle linear depolarization ratio. Measurements at 355 nm were performed with the ground-based Raman polarization lidars POLIS (Ludwigs-Maximilians-Universiät München) and with PollyXT of the Leibniz Institute for Tropospheric Research. Measurements were conducted during SAMUM-2 at Cape Verde (Saharan dust, marine, marine + dust and biomass burning + dust; Groß et al. (2011b)), in the framework of EARLINET in Leipzig, Germany (pollution; Illingworth and et al. (2014)) and in Munich, Germany (volcanic ash, transported dust; Groß et al. (2012); Wiegner et al. (2011), and in the Amazon Basin (fresh smoke; Baars et al. (2012)).

Figure 14 shows the particle linear depolarization ratio versus the lidar ratio at 355 nm and 532 nm of the different aerosol types which are, up to now, included in the aerosol classification schemes for EarthCARE (Illingworth and et al., 2014; Groß et al., 2015). Additionally we plotted our results found during the SALTRACE campaign for pure Saharan dust and for the boundary layer. Within the boundary layer our results fit quite well with former results found for marine aerosols or marine aerosol mixtures, indicating that the boundary layer was dominated by marine aerosols with various amount of dust mixed into the boundary layer on specific days. Regarding the Saharan dust layer one can see that the $\delta p - Sp$-space at 355 nm shows a good agreement to former dust measurements during SAMUM. The specified threshold of $0.23 \leq \delta_p \leq 0.33$ to identify pure Saharan dust from combined $\delta_p - S_p$ measurements (Groß et al., 2015) is still valuable for long-range transported dust. At 532 nm the SALTRACE results for long-range transported Saharan dust show slightly lower δ_p-values compared to the threshold ($\delta_p \geq 0.28$) used for the identification for Saharan dust (Groß et al., 2015). Thus this threshold has to be adapted to a slightly lower δ_p value of 0.26 to consider long-range transported Saharan dust.

5 Conclusions

We presented optical properties of Saharan dust long-range transported across the Atlantic Ocean to Barbados. For this purpose we analyzed measurements with the lidar system POLIS at 355 nm and 532 nm, in particular we calculated the extinction coefficient α_p, the lidar ratio S_p, and the particle linear depolarization ratio δ_p. While the first properties gives us information about the aerosol load, the latter two properties are intensive lidar properties and thus only dependent on the aerosol type and not on its amount. Therefore, these properties are used for aerosol classification schemes based on lidar measurements (Burton et al., 2012; Groß et al., 2013; Illingworth and et al., 2014; Groß et al., 2015). The measurements and results of this work follow up former measurements performed during the SAMUM-1 (Freudenthaler et al., 2009; Tesche et al., 2009b) and SAMUM-2 (Groß et al., 2011b; Tesche et al., 2011) campaigns and during a strong Saharan dust event over Central Europe observed in the framework of EARLINET (Wiegner et al., 2011). Thus, we are able to study possible changes of the optical properties of Saharan dust caused by long-range transport.

For the long-range transported Saharan dust over Barbados we found typical values of δ_p between 0.26 and 0.3 at 532 nm and between 0.24 and 0.29 at 355 nm. The mean systematic errors are 0.01 and 0.03 at 532 nm an 355 nm, respectively. Compared to δ_p-measurements at 532 nm during the SAMUM campaigns we see slightly lower values for long-range transported Saharan dust to Barbados, while over Central Europe slightly higher values have been found. This leads to the assumption that not only transport time but also the transport path, and the transport conditions have an influence of possible changes of the optical properties of Saharan dust. At 355 nm we do not see significant changes in the δ_p values although the overall mean values are slightly higher for long-range transported Saharan dust to Barbados as well as to Central Europe. For long-range transported Saharan dust we do not see a significant wavelength dependence anymore.

Mean values of the lidar ratio of the long-range transported Saharan dust over Barbados are 56 $\pm$ 7 sr at 532 nm and 53 $\pm$ 5 sr and thus agree well with the values found for fresh Saharan dust over Morocco (Tesche et al., 2009b). Although these values are slightly lower than the values found for long-range transported Saharan dust over Central Europe (Wiegner et al., 2011) and of mid-range transported Saharan dust over Cape Verde (Groß et al., 2011b) they agree for the measurement uncertainties. Thus we do not see a significant change in this optical properties during transport.

Though the presented measurements are a good test bed to study the optical properties of long-range transported Saharan dust, there are a number of questions remaining unsolved, e.g. the impact of transport condition on the changes of optical and microphysical properties. Thus further studies will combine lidar measurements with information of the transport conditions and path, e.g. from model calculations. Furthermore lidar measurements will be combined to in-situ measurements to get more inside the relationship between optical and microphysical properties, e.g. the cloud condensation properties, and about a possible vertical sorting within the dust layer as recently suggested by Yang et al. (2013).

Acknowledgements. This work has been partly funded by the Deutsche Forschungsgemeinschaft (DFG) in the SPP (no. 1294/2) "‘Atmosphären- und Erdsystemforschung mit dem Forschungsflugzeug HALO (High Altitude and Long Range Research Aircraft)"’ under contract no. KI1567/1-1, and by the Helmholtz Association under grant number VH-NG-606 (Helmholtz-Hochschul-Nachwuchsforschergruppe AerCARE). The SALTRACE campaign was mainly funded by the Helmholtz Association, the Deutsches Zentrum für Luft- und Raumfahrt (DLR), the Ludwig-Maximilians-Universität München (LMU), and the Institut für Troposphärenforschung (TROPOS). CIMEL calibration was performed at the AERONET-EUROPE calibration center at GOA-UVA, supported by ACTRIS (European Union Seventh Framework Program, FP7/2007-2013) under grant agreement no. 262254. The lidar and sun-photometer measurements were performed at the site of the Caribbean Institute for Meteorology and Hydrology (CIMH). We thank CIMH for providing us this measurement environment.

References

Amiridis, V., Balis, D. S., Giannakaki, E., Stohl, A., Kazadzis, S., Koukouli, M. E., and Zanis, P.: Optical characteristics of biomass burning aerosols over Southeastern Europe determined from UV-Raman lidar measurements, Atmospheric Chemistry and Physics, 9, 2431–2440, doi:10.5194/acp-9-2431-2009, http://www.atmos-chem-phys.net/9/2431/2009/, 2009.

Ansmann, A., Riebensell, M., and Weitkamp, C.: Measurement of atmospheric aerosol extinction profiles with a Raman lidar, Opt. Lett., 14, 746–748, 1990.

Ansmann, A., Wandinger, U., Riebesell, M., Weitkamp, C., and Michaelis, W.: Independent measurement of extinction and backscatter profiles in cirrus clouds by using a combined Raman elastic-backscatter lidar, Applied Optics, 31, 7113–7113, doi:10.1364/AO.31.007113, http://ao.osa.org/abstract.cfm?URI=ao-31-33-7113, 1992.

Ansmann, A., Petzold, A., Kandler, K., Tegen, I., Manfred, W., Müller, D., Weinzierl, B., Müller, T., and Heintzenberg, J.: Saharan Mineral Dust Experiments SAMUM-1 and SAMUM-2: what have we learned?, Tellus B, 63, 403–429, doi:10.1111/j.1600-0889.2011.00555.x, http://dx.doi.org/10.1111/j.1600-0889.2011.00555.x, 2011.

Baars, H., Ansmann, A., Althausen, D., Engelmann, R., Heese, B., Müller, D., Artaxo, P., Paixao, M., Pauliquevis, T., and Souza, R.: Aerosol profiling with lidar in the Amazon Basin during the wet and dry season, Journal of Geophysical Research: Atmospheres, 117, n/a–n/a, doi:10.1029/2012JD018338, http://dx.doi.org/10.1029/2012JD018338, d21201, 2012.

Bauer, S. E., Mishchenko, M. I., Lacis, A. A., Zhang, S., Perlwitz, J., and Metzger, S. M.: Do sulfate and nitrate coatings on mineral dust have important effects on radiative properties and climate modeling?, Journal of Geophysical Research: Atmospheres, 112, n/a–n/a, doi:10.1029/2005JD006977, http://dx.doi.org/10.1029/2005JD006977, d06307, 2007.

Biele, J., Beyerle, G., and Baumgarten, G.: Polarization Lidar: Correction of instrumental effects, Opt. Express, 7, 427–435, doi:10.1364/OE.7.000427, http://www.opticsexpress.org/abstract.cfm?URI=oe-7-12-427, 2000.

Boucher, O., an P. Artaxo, D. R., Bretherton, C., Feingold, G., Forster, P., Keminen, V.-M., Kondo, Y., Liao, H., Lohmann, U., Rasch, P., Satheesh, S., Sherwood, S., Stevens, B., and Zhang, X. Y.: Clouds and Aerosols. In Climate Change 2013: The Physical Science Basis. Contribution of Working Group I to the Fifth Assessment Report of the Intergovernmental Panel on Climate Change, Cambridge University Press, pp. 571–657, 2013.

Burton, S. P., Ferrare, R. A., Hostetler, C. A., Hair, J. W., Rogers, R. R., Obland, M. D., Butler, C. F., Cook, A. L., Harper, D. B., and Froyd, K. D.: Aerosol classification using airborne High Spectral Resolution Lidar measurements - methodology and examples, Atmospheric Measurement Techniques, 5, 73–98, doi:10.5194/amt-5-73-2012, http://www.atmos-meas-tech.net/5/73/2012/, 2012.

Cattrall, C., Reagan, J., Thome, K., and Dubovik, O.: Variability of aerosol and spectral lidar and backscatter and extinction ratios of key aerosol types derived from selected Aerosol Robotic Network locations, Journal of Geophysical Research, 110, D10S11, doi:10.1029/2004JD005124, 2005.

Draxler, R. R. and Rolph, G. D.: HYSPLIT (HYbrid Single Particle Lagrangian Integrated Trajectory) Model, NOAA Air Resources Laboratory, Silver Spring, MD, http://ready.arl.noaa.gov/HYSPLIT.php, 2012.

Forster, P. and et al.: Changes in atmospheric constituents and in radiative forcing, Climate Change 2007: The Physical Science Basis. Contribution of Working Group I to the Fourth Assessment Report of the Intergovernmental Panel on Climate Change, Cambridge University Press, pp. 210–215, 2007.

Freudenthaler, V., Esselborn, M., Wiegner, M., Heese, B., Tesche, M., Ansmann, A., Müller, D., Althause, D., Wirth, M., Fix, A., Ehret, G., Knippertz, P., Toledano, C., Gasteiger, J., Garhammer, M., and Seefeldner, M.: Depolarization ratio profiling at several wavelengths in pure Saharan dust during SAMUM 2006., Tellus B, 61, 165–179, 2009.

Freudenthaler, V., Seefeldner, M., Groß, S., and Wandinger, U.: Accuracy of linear depolarisation ratios in clean air ranges measured with POLIS-6 at 355 and 532 nm., Proceeding of 27. International Laser Radar Conference, New York, 2015.

Gasteiger, J., Groß, S., Freudenthaler, V., and Wiegner, M.: Volcanic ash from Iceland over Munich: mass concentration retrieved from ground-based remote sensing measurements, Atmospheric Chemistry and Physics, 11, 2209–2223, doi:10.5194/acp-11-2209-2011, http://www.atmos-chem-phys.net/11/2209/2011/, 2011a.

Gasteiger, J., Wiegner, M., Groß, S., Freudenthaler, V. Toledano, C., Tesche, M., and Kandler, K.: Modeling lidar-relevant optical properties of complex mineral dust aerosols, Tellus B, 63, 2011b.

Goudie, A. and Middleton, N.: Saharan dust storms: nature and consequences., Earth-Science Reviews, 56, 179–204, 2001.

Groß, Freudenthaler, V., Wirth, M., and Weinzierl, B.: Towards an aerosol classification scheme for future EarthCARE lidar observations and implications for research needs, Atmospheric Science Letters, 16, 77–82, doi:10.1002/asl2.524, http://dx.doi.org/10.1002/asl2.524, 2015.

Groß, S., Gasteiger, J., Freudenthaler, V., Wiegner, M., Geiß, A., Toledano, C., Kandler, K., Tesche, M., Ansmann, A., and Wiedensohler, A.: Characterization of the planetary boundary layer during SAMUM-2 by means of lidar measurements, Tellus, B 63, 695–705, 2011a.

Groß, S., Tesche, M., Freudenthaler, V., Toledano, C., Wiegner, M., Ansmann, A., Althausen, D., and Seefeldner, M.: Characterization of Saharan dust, marine aerosols and mixtures of biomass burning aerosols and dust by means of multi-wavelength depolarization- and Raman-measurments during SAMUM-2, Tellus B, 63, 706 – 724, doi:10.1111/j.1600-0889.2011.00556.x, tellus B63, 2011b.

Groß, S., Wiegner, M., Freudenthaler, V., and Toledano, C.: Lidar ratio of Saharan dust over Cape Verde Islands: Assessment and error calculation, Journal of Geophysical Research: Atmospheres, 116, n/a–n/a, doi:10.1029/2010JD015435, http://dx.doi.org/10.1029/2010JD015435, d15203, 2011c.

Groß, S., Freudenthaler, V., Wiegner, M., Gasteiger, J., Geiß, A., and Schnell, F.: Dual-wavelength linear depolarization ratio of volcanic aerosols: Lidar measurements of the Eyjafjallajökull plume over Maisach, Germany, Atmospheric Environment, 48, 85 – 96, doi:http://dx.doi.org/10.1016/j.atmosenv.2011.06.017, http://www.sciencedirect.com/science/article/pii/S1352231011006108, volcanic ash over Europe during the eruption of Eyjafjallajökull on Iceland, April-May 2010, 2012.

Groß, S., Esselborn, M., Weinzierl, B., Wirth, M., Fix, A., and Petzold, A.: Aerosol classification by airborne high spectral resolution lidar observations, Atmospheric Chemistry and Physics, 13, 2487–2505, doi:10.5194/acp-13-2487-2013, http://www.atmos-chem-phys.net/13/2487/2013/, 2013.

Groß, S., Wirth, M., Schäfler, A., Fix, A., Kaufmann, S., and Voigt, C.: Potential of airborne lidar measurements for cirrus cloud studies, Atmospheric Measurement Techniques, 7, 2745–2755, doi:10.5194/amt-7-2745-2014, http://www.atmos-meas-tech.net/7/2745/2014/, 2014.

Haywood, J. and Boucher, O.: Estimates of the direct and indirect radiative forcing due to tropospheric aerosols: a review., Rev. of Geophysics, 38, 513–543, 2000.

Holben, B., Eck, T., Slutsker, I., Tanré, D., Buis, J., Setzer, A., Vermote, E., Reagan, J., Kaufman, Y., Nakajima, T., Lavenu, F., Jankowiak, I., and Smirnov, A.: AERONET–A Federated Instrument Network and Data Archive for Aerosol Characterization, Remote Sensing of Environment, 66, 1 – 16, doi:10.1016/S0034-4257(98)00031-5, http://www.sciencedirect.com/science/article/B6V6V-3V7SF8D-1D/2/7452854b09ed6f6d885f0aa14ac67ed6, 1998.

Illingworth, A. J. and et al.: THE EARTHCARE SATELLITE: The next step forward in global measurements of clouds, aerosols, precipitation and radiation., Bulletin of the American Meteorological Society, e-View, 2014.

IPCC: climate Change 2013: The Scientific Basis., Cambridge University Press, 2013.

Liu, Z., Omar, A., Vaughan, M., Hair, J., Kittaka, C., Hu, Y., Powell, K., Trepte, C., Winker, D., Hostetler, C., Ferrare, R., and Pierce, R.: Calipso lidar observations of the optical properties of saharan dust: A case study of long-range transport, Journal of Geophysical Research, 113, D07 207+, 2008.

Müller, D., Ansmann, A., Mattis, I., Tesche, M., Wandinger, U., Althausen, D., and Pisani, G.: Aerosol-type-dependent lidar ratios observed with Raman lidar, Journal of Geophysical Research, 112, D16 202, doi:10.1029/2006JD008292, 2007.

Nousiainen, T.: Optical modeling of mineral dust particles: A review, Journal of Quantitative Spectroscopy and Radiative Transfer, 110, 1261 – 1279, doi:http://dx.doi.org/10.1016/j.jqsrt.2009.03.002, http://www.sciencedirect.com/science/article/pii/S0022407309000934, {XI} Conference on Electromagnetic and Light Scattering by Non-Spherical Particles: 2008, 2009.

Omar, A., Winker, D., Kittaka, C., Vaughan, M., Liu, Z., Hu, Y., Trepte, C., Rogers, R., Ferrare, R., Lee, K., Kuehn, R., and Hostetler, C.: The CALIPSO Automated Aerosol Classification and Lidar Ratio Selection Algorithm, Journal of Atmospheric Oceanic Technologie, 26, 1994—-2014, 2009.

Penner, J. E. and et al.: Climate change 2001: The scientific assessment, Cambridge Univ. Press, pp. 289–348, 2001.

Penner, J. E., Xu, L., and Wang, M.: Satellite methods underestimate indirect climate forcing by aerosols, Proceedings of the National Academy of Sciences, 108(33)), 13,404–13,408, 2011.

Piironen, P. and Eloranta, E. W.: Demonstration of a high-spectral-resolution lidar based on an iodine absorption filter, Opt. Lett., 19, 234–236, doi:10.1364/OL.19.000234, http://ol.osa.org/abstract.cfm?URI=ol-19-3-234, 1994.

Prospero, J. M., Bonatti, E., Schubert, C., and Carlson, T. N.: Dust in the Caribbean atmosphere traced to an African dust storm, Earth and Planetary Science Letters, 9, 287 – 293, doi:http://dx.doi.org/10.1016/0012-821X(70)90039-7, http://www.sciencedirect.com/science/article/pii/0012821X70900397, 1970.

Redmond, H. E., Dial, K. D., and Thompson, J. E.: Light scattering and absorption by wind blown dust: Theory, measurement, and recent data, Aeolian Research, 2, 5 – 26, doi:http://dx.doi.org/10.1016/j.aeolia.2009.09.002, http://www.sciencedirect.com/science/article/pii/S1875963709000317, 2010.

Sakai, T., Nagai, T., Zaizen, Y., and Mano, Y.: Backscattering linear depolarization ratio measurements of mineral, sea-salt, and ammonium sulfate particles simulated in a laboratory chamber, Applied Optics, 49, 4441–4449, doi:10.1364/AO.49.004441, http://ao.osa.org/abstract.cfm?URI=ao-49-23-4441, 2010.

Sassen, K., Zhao, H., and Yu, B.-K.: Backscatter laser depolarization studies of simulated stratospheric aerosols: crystallized sulfuric acid droplets, Applied Optics, 28, 3024–3029, doi:10.1364/AO.28.003024, http://ao.osa.org/abstract.cfm?URI=ao-28-15-3024, 1989.

Schepanski, K., Tegen, I., Laurent, B., Heinold, B., and Macke, A.: A new Saharan dust source activation frequency map derived from MSG-SEVIRI IR-channels, Geophys. Res. Lett., 34, L18 803, doi:10.1029/2007GL03168, 2007.

Schuster, G. L., Vaughan, M., MacDonnell, D., Su, W., Winker, D., Dubovik, O., Lapyonok, T., and Trepte, C.: Comparison of CALIPSO aerosol optical depth retrievals to AERONET measurements, and a climatology for the lidar ratio of dust, Atmospheric Chemistry and Physics, 12, 7431–7452, doi:10.5194/acp-12-7431-2012, http://www.atmos-chem-phys.net/12/7431/2012/, 2012.

Shao, Y., Wyrwoll, K.-H., Chappell, A., Huang, J., Lin, Z., McTainsh, G. H., Mikami, M., Tanaka, T. Y., Wang, X., and Yoon, S.: Dust cycle: An emerging core theme in Earth system science, Aeolian Research, 2, 181 – 204, doi:http://dx.doi.org/10.1016/j.aeolia.2011.02.001, http://www.sciencedirect.com/science/article/pii/S1875963711000085, 2011.

Shimizu, A., Sugimoto, N., Matsui, I., Arao, K., Uno, I., Murayama, T., Kagawa, N., Aoki, K., Uchiyama, A., and Yamazaki, A.: Continuous observations of Asian dust and other aerosols by polarization lidar in China and Japan during ACE-Asia, Journal of Geophysical Research, 109, D19S17, doi:10.1029/2002JD003253, 2004.

Shimizu, H., Lee, S., and She, C.: High spectral resolution lidar system with atomic blocking filters for measuring atmospheric parameters, Applied Optics, 22, 1373–1381, doi:10.1364/AO.22.001373, http://ao.osa.org/abstract.cfm?URI=ao-22-9-1373, 1983.

Shipley, S., Tracy, D., Eloranta, E., Trauger, J., Sroga, J., Roesler, F., and Weinman, J.: High spectral resolution lidar to measure optical scattering properties of atmospheric aerosols. 1: Theory and instrumentation, Applied Optics, 22, 3716–3724, doi:10.1364/AO.22.003716, http://ao.osa.org/abstract.cfm?URI=ao-22-23-3716, 1983.

Su, W., Loeb, N. G., Schuster, G. L., Chin, M., and Rose, F. G.: Global all-sky shortwave direct radiative forcing of anthropogenic aerosols from combined satellite observations and GOCART simulations, Journal of Geophysical Research: Atmospheres, 118, 655–669, doi:10.1029/2012JD018294, http://dx.doi.org/10.1029/2012JD018294, 2013.

Tesche, M., Ansmann, A., Müller, D., Althausen, D., Engelmann, R., Freudenthaler, V., and Groß, S.: Vertically resolved separation of dust and smoke over Cape Verde using multiwavelength Raman and polarization lidars during Saharan Mineral Dust Experiment 2008, Journal of Geophysical Research, 114, D13 202, 2009a.

Tesche, M., Ansmann, A., Müller, D., Althausen, D., Mattis, I., Heese, B., Freudenthaler, V., Wiegner, M., Esselborn, M., Pisani, G., and Knippertz, P.: Vertical profiling of Saharan dust with Raman lidars and airborne HSRL in southern Morocco during SAMUM, Tellus, B 61, 144–164, 2009b.

Tesche, M., Gross, S., Ansmann, A., Müller, D., Althause, D., Freudenthaler, V., and Esselborn, M.: Profiling of Saharan dust and biomass-burning smoke with multiwavelength polarization Raman lidar at Cape Verde, Tellus, B 63, 649–676, doi:10.1111/j.1600-0889.2011.00548.x, 2011.

Washington, R., Todd, M., Middleton, N. J., and Goudie, A. S.: Dust-Storm Source Areas Determined by the Total Ozone Monitoring Spectrometer and Surface Observations, Annals of the Association of American Geographers, 93, 297–313, 2003.

Weinzierl, B., Sauer, D., Esselborn, M., Petzold, A., Mund, S., Veira, A., Tesche, M., Ansmann, A., and Wirth, M.: Airborne observations of microphysical and optical properties of dust and biomass burning aerosol layers in the Cape Verde region during SAMUM 2008., Tellus, B 63, 2011.

Wiegner, M., Groß, S., Freudenthaler, V., Schnell, F., and Gasteiger, J., : The May/June 2008 Saharan dust event over Munich: Intensive aerosol parameters from lidar measurements, Journal of Geophysical Research: Atmospheres , 116, D23, 2011.

Winker, D. M., Vaughan, M. A., Omar, A., Hu, X., Powell, K. A., Liu, Z., Hund, W. H., and Young, S. A.: Overview of the CALIPSO Mission and CALIOP Data Processing Algorithms, J. Atmos. Oceanic Technol., 26, 2310–2323, doi:http://dx.doi.org/10.1175/2009JTECHA1281.1, 2009.

Yang, W., Marshak, A., Kostinski, A. B., and Várnai, T.: Shape-induced gravitational sorting of Saharan dust during transatlantic voyage: Evidence from CALIOP lidar depolarization measurements, Geophysical Research Letters, 40, 3281–3286, doi:10.1002/grl.50603, http://dx.doi.org/10.1002/grl.50603, 2013.